

Synthesis of Monodisperse, Highly Emissive, and Size-Tunable Cd₃P₂ Nanocrystals

Renguo Xie,^{*,†,‡} Jiexian Zhang,[†] Fei Zhao,[‡]
Wensheng Yang,[†] and Xiaogang Peng[‡]

[†]College of Chemistry, Jilin University, Changchun, Jilin Province 130021, P. R. China, and [‡]Department of Chemistry and Biochemistry, University of Arkansas, Fayetteville, Arkansas 72701

Received March 27, 2010

Revised Manuscript Received May 19, 2010

Colloidal semiconductor nanocrystals have been extensively explored because of their excellent optical and optoelectronic properties.¹ However, success on synthesis of high-quality semiconductor nanocrystals have been largely limited to II–VI² ones, followed by IV–VI,³ III–V,⁴ and I–III–VI⁵ ones. Although II–V semiconductors, such as Cd₃P₂ and Cd₃As₂, possess great potential in comparison to the others, II–V semiconductors nanocrystals have been lagging far behind in terms of their synthetic chemistry. For example, Cd₃P₂ as a representative II–V semiconductor, its band gap is 0.55 eV and large excitonic radii is quite large 18 nm.⁶ Correspondingly, Cd₃P₂ nanocrystals should exhibit tunable optical and optoelectronic properties in a wide size range (up to 18 nm)⁷ and have great potential in infrared (IR) detectors, ultrasonic multipliers, solar cells etc.⁸

Although physical method is successful on preparation of II–V semiconductor nanomaterials,⁹ there were only a

few reports on synthesis of colloidal Cd₃P₂ nanocrystals by wet chemistry routes,¹⁰ precipitation of cadmium ion by PH₃ in aqueous solution, thermolysis of single-source precursor [MeCdPBu₂]₃ or employment of metal–organic precursors Me₂Cd and HPbu₂ in tri-*n*-octylphosphine oxide (TOPO). Usually, size of the Cd₃P₂ particles obtained by these approaches was quite narrow, in the range from 2 to 3 nm, which showed band gap emission from 550 to 680 nm.^{10c–e}

Here, we report synthesis of nearly monodispersed Cd₃P₂ nanocrystals in a large size range (between 1.6 and 12 nm) in octadecene (ODE). A typical synthesis is as follows: 0.3 mmol CdO, 4 mL ODE, and 1 mmol oleic acid (OA) were loaded into a 25 mL three-necked flask and heated to 230 °C under Ar flow (no vacuum pumping). Into this solution was quickly injected 0.1 mmol tris-trimethylsilyl phosphine (TMS-P) dissolved in 0.5 mL ODE. Subsequently, the growth of Cd₃P₂ nanocrystals was set at 250 °C. No size sorting was applied to any sample used for characterization in this work.

Transmission electron microscope (TEM) images of three typical samples are given in Figure 1A–C (also see the Supporting Information, Figure 1S) and a square array of the nanocrystals is observed (Figure 1C). Though it was difficult to identify a faceted shape in the small nanocrystals (<8 nm), the relatively large ones possessed square or rectangular shapes (see the Supporting Information, Figure S1). All the nanocrystals were nearly monodispersed (polydispersity <10%). A representative lattice-resolved high-resolution TEM (HRTEM) image of the Cd₃P₂ nanocrystals is given in Figure 3D. The clearly marked interplanar *d* spacing is 0.311 nm, which corresponds to that of the {220} lattice planes of tetragonal Cd₃P₂. Further HRTEM analysis (see Figure S2 in the Supporting Information) reveals the three dimensions of a tetragonal Cd₃P₂ nanocrystal was length × width × height = 12 nm × 12 nm × 6 nm). With the aid of XRD data (Figure 1E), the crystalline structure of the Cd₃P₂ nanocrystals is clearly confirmed (Figure 1E), which is indexed based on a primitive tetragonal symmetry (space group *P42/nmc*, *a* = 0.872 nm, *c* = 1.2347 nm) and matches well with the expected lattice parameters for single-crystal Cd₃P₂ films. Electron dispersion spectroscopy (EDS) spectra of the purified products (see the Supporting Information, Figure S3) reveals that the sample is composed of Cd and P atoms with an approximate atomic ratio of 1.56:1.00, close to the stoichiometry of Cd₃P₂.

All reactions for synthesizing different size Cd₃P₂ nanocrystals were performed under the identical conditions except for the concentration of OA in the reaction

*Corresponding author.

- (1) (a) Alivisatos, A. P. *Science* **1996**, *271*, 933. (b) Efras, A.; Rosen, M. *Annu. Rev. Mater. Sci.* **2000**, *30*, 473. (c) Burda, C.; Chen, X.; Narayanan, R.; El-Sayed, M. A. *Chem. Rev.* **2005**, *105*, 1025. (d) Talapin, D. V.; Murray, C. B. *Science* **2005**, *310*, 86.
- (2) (a) Murray, C. B.; Norris, D. J.; Bawendi, M. G. *J. Am. Chem. Soc.* **1993**, *115*, 8706. (b) Yu, W. W.; Peng, X. G. *Angew. Chem., Int. Ed.* **2002**, *41*, 2368.
- (3) (a) Hines, M. A.; Scholes, G. D. *Adv. Mater.* **2003**, *15*, 1844. (b) Mokari, T.; Zhang, M.; Yang, P. D. *J. Am. Chem. Soc.* **2007**, *129*, 9864.
- (4) (a) Cao, Y. W.; Banin, U. *J. Am. Chem. Soc.* **2000**, *122*, 9692. (b) Xie, R. G.; Battaglia, D.; Peng, X. G. *J. Am. Chem. Soc.* **2007**, *129*, 15432. (c) Xie, R. G.; Peng, X. G. *Angew. Chem., Int. Ed.* **2008**, *47*, 7677.
- (5) (a) Wang, D. S.; Zheng, W.; Hao, C. H.; Peng, Q.; Li, Y. D. *Chem. Commun.* **2008**, 2556. (b) Pan, D. C.; An, L. J.; Sun, Z. M.; Hou, W.; Yang, Y.; Yang, Z. Z.; Lu, Y. F. *J. Am. Chem. Soc.* **2008**, *130*, 5620. (c) Xie, R. G.; Peng, X. G. *J. Am. Chem. Soc.* **2009**, *131*, 5691.
- (6) (a) Lin-Chung, P. *J. Phys. Status Solidi B* **1971**, *47*, 33. (b) Sieranski, K.; Sztarkowski, J.; Misiewicz, J. *Phys. Rev. B* **1994**, *50*, 7331.
- (7) (a) Jay-Gerin, J. P.; Aubin, M. J.; Caron, L. G. *Phys. Rev. B* **1978**, *18*, 5675. (b) Nozik, A. J.; Williams, F.; Nenadovic, M. I.; Rajh, T.; Micic, O. I. *J. Phys. Chem.* **1985**, *89*, 397.
- (8) (a) Bishop, S. G.; Moore, W. J.; Swiggard, E. M. *Appl. Phys. Lett.* **1970**, *16*, 459. (b) Zdanowicz, W.; Zdanowicz, L. *Annu. Rev. Mater. Sci.* **1975**, *5*, 1. (c) Pawlikowski, J. M. *Infra-Red Phys.* **1988**, *28*, 177. (d) Hermann, A. M.; Madan, A.; Wanlass, M.; Badri, V.; Ahrenkiel, R.; Morrison, S.; Gonzales, C. *Sol. Energy Mater. Sol. Cells* **2004**, *82*, 241. (e) Shen, G.; Chen, P.; Bando, Y.; Golberg, D.; Zhou, C. *Chem. Mater.* **2008**, *20*, 731.
- (9) (a) Shen, G.; Bando, Y.; Ye, C.; Yuan, X.; Sekiguchi, T.; Golberg, D. *Angew. Chem., Int. Ed.* **2006**, *45*, 7568. (b) Shen, G.; Bando, Y.; Golberg, D. *J. Phys. Chem. C* **2007**, *111*, 5044.

- (10) (a) Goel, S. C.; Chang, M. Y.; E. Buhro, W. *J. Am. Chem. Soc.* **1990**, *112*, 5636. (b) Matchett, M. A.; Viano, A. M.; Adolph, N. L.; Stoddard, R. D.; Buhro, W. E.; Conradi, M. S.; Gibson, P. C. *Chem. Mater.* **1992**, *4*, 508. (c) Kornowski, A.; Eichberger, R.; Giersig, M.; Weller, H.; Eychmuller, A. *J. Phys. Chem.* **1996**, *100*, 12467. (d) Green, M.; O'Brien, P. *Adv. Mater.* **1998**, *10*, 527. (e) Green, M.; O'Brien, P. *J. Mater. Chem.* **1999**, *9*, 243. (f) Wang, R.; Ratcliffe, C. I.; Wu, X.; Voznyy, O.; Tao, Y.; Yu, K. *J. Phys. Chem. C* **2009**, *113*, 17979.

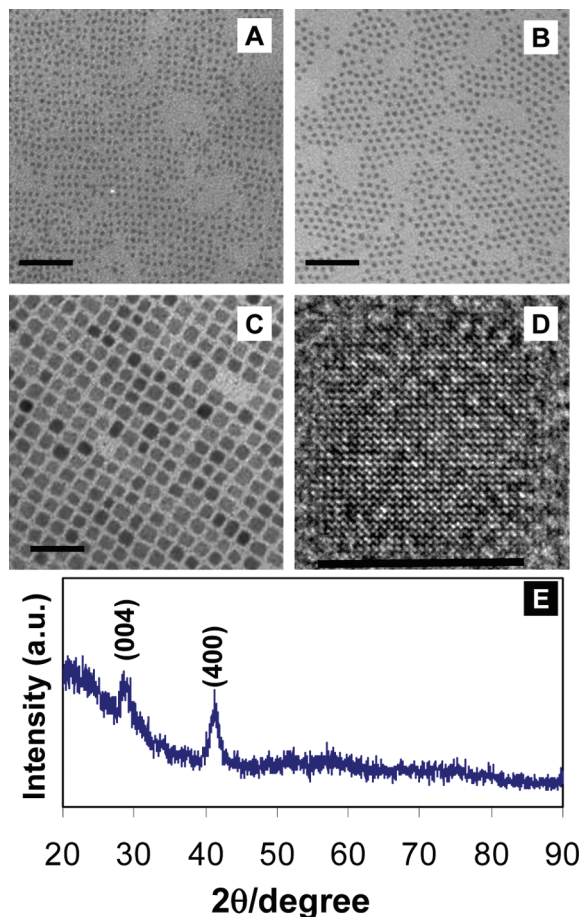


Figure 1. TEM images of Cd_3P_2 nanocrystals with different sizes: (A) 2.5, (B) 4.0, and (C) 12 nm. HR-TEM image (D) of Cd_3P_2 nanocrystals (sample in C). (E) X-ray diffraction pattern (XRD) of Cd_3P_2 nanocrystals (sample in C). Scale bar is 50 nm for TEM and 10 nm for HRTEM.

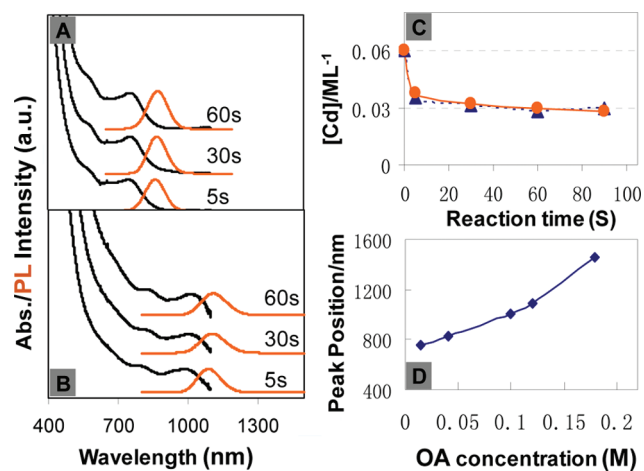


Figure 2. Temporal evolution of UV-vis-NIR (black) and PL spectra (red) of Cd_3P_2 nanocrystals synthesized under different concentration of OA: (A) 0.015 and (B) 0.1 mM. (C) Temporal evolution of the monomer concentrations with the reaction time under OA concentration of 0.015 (black) and 0.1 mM (red), respectively. (D) OA concentration-dependent absorption peak position of Cd_3P_2 nanocrystals.

mixtures. Figure 2 illustrates the temporal evolution of the optical properties of Cd_3P_2 nanocrystals under different concentrations of OA. It was noted that the reachable size range for one reaction was limited, as indicated

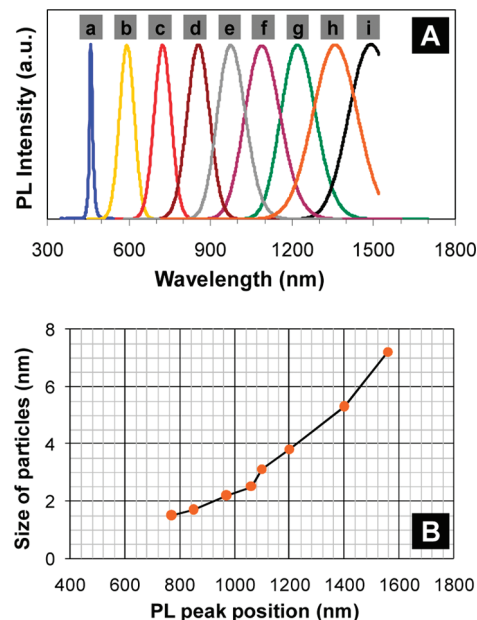


Figure 3. (A) Photoluminescence spectra of Cd_3P_2 nanocrystals with various sizes. (a) < 1.5, (b) < 1.5, (c) 1.5, (d) 1.8, (e) 2.4, (f) 3, (g) 4, (h) 5.5, and (i) 7.6 nm. (B) Relation between the size of Cd_3P_2 nanocrystals and their emission peak positions.

by nearly time-independent absorption and photoluminescence (PL) spectra. However, the size of the nanocrystals could be tuned from 1.6 to over 12 nm by increasing the OA concentration from 0.25 to 0.4 mM (see Figure S1 in the Supporting Information and Figure 2D).

A similar solution system was employed for the synthesis of high-quality CdS (II–VI) and InAs (III–V) nanocrystals previously. In the case of CdS nanocrystals, the OA concentration could tune the size of the nanocrystals in a certain extent but the size of the nanocrystals in a given reaction was found to be nearly invariable.^{2b} Conversely, the InAs nanocrystals almost showed no dependence of the OA concentration.^{4c} The kinetics for the growth of Cd_3P_2 nanocrystals observed here is substantially different from that observed for the CdS and InAs ones. To further understand the influence of the OA concentration on the growth of Cd_3P_2 nanocrystals, the concentration of the cadmium monomers in the solution were determined after the injection of TMS-P into the reaction solutions. Figure 2C presents the temporal evolution of the cadmium monomer concentration for two reactions. One can find that the concentration of cadmium monomer quickly decreased 30 s after the TMS-P injection, and then kept almost constant. According to the molar ratio of Cd and P used (3: 1), half of Cd^{2+} should be consumed at the end of both reactions. Therefore, it is reasonable to conclude that the reactions underwent almost completely in 30 s, indicating that Cd_3P_2 nanocrystals with different sizes could be successfully synthesized within 30 s by simply changing the concentration of OA. From the data discussed in these paragraphs, it is deduced that the number of the nanocrystals formed at the initial formation stage decreased with increasing the OA concentration. This is consistent with a reaction-controlled formation model.¹¹

(11) Xie, R. G.; Li, Z.; Peng, X. G. *J. Am. Chem. Soc.* **2009**, *131*, 15457.

The Cd_3P_2 nanocrystals smaller than 7.6 nm were identified to exhibit strong and narrow band-edge PL with quantum yields higher than 30%, which covers the whole visible and near-IR (450 to over 1500 nm) region (Figure 3A). For the 2–3 nm nanocrystals, the quantum yield is as high as 70%. Even for the extremely small-sized Cd_3P_2 nanocrystals, the quantum yield can reach up to 35%. A photograph of several samples emitting (Figure 3Aa–d) from blue to NIR are shown in Figure S5 in the Supporting Information. It should be noted that when the size of the nanocrystals is over 8 nm, the PL could not be recorded with the instrument limitation in our laboratory. The relationship of Cd_3P_2 nanocrystal sizes (below 8 nm) versus their emission peak positions are summarized in Figure 3B. In principle, a wider emission window of Cd_3P_2 nanocrystals should be observable because of their large Bohr radii, which is comparable with InAs nanocrystals but much broader than typical II–VI ones.

In conclusion, a “simple and quick” synthetic scheme has been developed for synthesis of high quality Cd_3P_2

nanocrystals with controllable sizes in a wide range from below 1.6 to 12 nm by simply adjusting the OA concentration in solution. The as-prepared Cd_3P_2 nanocrystals exhibit strong band gap PL with quantum yield higher than 30%. The emission window of the nanocrystals covers the whole visible and NIR range (450 to over 1500 nm). The interesting optical properties make the nanocrystals potentially useful in telecommunication, optical amplification, and lighting. The current synthetic approach would open a new route for the synthesis of other high-quality II–V semiconductor nanocrystals.

Acknowledgment. This work was supported by the National Natural Science Foundation of China (50825202) and the Program for NCET in University of Chinese Ministry of Education.

Supporting Information Available: Detailed experimental procedures and additional figures (PDF). This material is available free of charge via the Internet at <http://pubs.acs.org>